JCTC Journal of Chemical Theory and Computation

Equilibrium Geometries of Noncovalently Bound Intermolecular Complexes Derived from Subsystem Formulation of Density Functional Theory†

Marcin Dułak,‡ Jakub W. Kamiński,*,‡,§ and Tomasz A. Wesołowski‡

Département de Chimie Physique, Université de Genève, 30, quai Ernest-Ansermet, CH-1211 Genève 4, Switzerland, and Institute of Physical and Theoretical Chemistry, Wrocław University of Technology, Wyb. Wyspiańskiego 27, 50-370 Wrocław, Poland

Received December 18, 2006

Abstract: The subsystem formulation of density functional theory is used to obtain equilibrium geometries and interaction energies for a representative set of noncovalently bound intermolecular complexes. The results are compared with literature benchmark data. The range of applicability of two considered approximations to the exchange-correlation- and nonadditive kinetic energy components of the total energy is determined. Local density approximation, which does not involve any empirical parameters, leads to excellent intermolecular equilibrium distances for hydrogen-bonded complexes (maximal error 0.13 Å for NH_3-NH_3). It is a method of choice for a wide class of weak intermolecular complexes including also dipole-bound and the ones formed by rare gas atoms or saturated hydrocarbons. The range of applicability of the chosen generalized gradient approximation, which was shown in our previous works to lead to good interaction energies in such complexes, where π-electrons are involved in the interaction, remains limited to this group because it improves neither binding energies nor equilibrium geometries in the wide class of complexes for which local density approximation is adequate. An efficient energy minimization procedure, in which optimization of the geometry and the electron density of each subsystem is made simultaneously, is proposed and tested.

1. Introduction

The principal motivation for this work originates in our interest in the *orbital-free embedding* formalism[1] to study environment-induced changes of the electronic structure of an embedded species: localized electronic excitations,[2,3] hyperfine tensor,[4] dipole moments,[5] *f*-levels,[6] and the gap between the high- and low spin potential energy surfaces,[7] for instance. In the orbital-free embedding calculations, all the information about the environment is confined in its electron density, and only the selected subsystem is described at the orbital level.

The quality of such properties of the total system as electron density distribution, total energy, response properties, etc., derived from the orbital-free embedding calculations is determined by the following two factors: the use of approximate density functionals for exchange-correlation- and nonadditive kinetic energy instead of the corresponding exact quantities (see the Methods section below) and the choice of the electron density corresponding to the environment, which is derived from some other methods involving lower computational costs. Whereas the accuracy of the used functionals cannot be controlled in a straightforward manner (their exact forms are known only for some systems), the effect of the choice of the electron density of the environment can be easily verified in practice because the electron density assigned to the environment can be also subject of optimization. The process of minimization of the total energy with respect to both components of the total electron density can

† Dedicated to Dennis R. Salahub on the occasion of his 60th birthday.

* Corresponding author e-mail: Jakub.Kaminski@chiphy.unige.ch.
‡ Université de Genève.
§ Wrocław University of Technology.

10.1021/ct600367t CCC: $37.00
Published on Web 03/15/2007

proceed as a series of partial minimization steps (*freeze-and-thaw* cycle), in which both subsystems exchange their roles until minimum is reached.[8] Of course, both subsystems are treated on equal footing, and the notion of *environment* and *embedded subsystem* loses its meaning at the end of such minimization procedure. Fully variational calculations represent numerical implementation of the subsystem formulation of density functional theory (DFT) introduced by Cortona.[9]

In the multilevel computer simulations applying orbital-free embedding formalism, fully variational calculations can be applied as a complementary tool to assess the adequacy of the electron density chosen to represent the environment. For instance, the effect of relaxation of the electron density of the environment in model systems was reported in several previous publications.[2−4,6]

This work concerns the source of errors in orbital-free embedding calculations arising from the use of approximate density functionals for exchange-correlation and nonadditive kinetic energies. To this end, the subsystem formulation of DFT is used to minimize the total energy with respect to electron densities of both subsystems in a representative sample of weakly interacting intermolecular complexes. Compared to investigations of the adequacy of the applied density functional reported previously, we focus the analysis not on interaction energies only but on equilibrium geometries.

The effect of the environment on the electronic structure of the embedded subsystem can be seen as the result of two effects: the environment induced changes of the geometry and the direct electronic effects (for a recent representative analysis, see ref 10). In many cases, the geometry of the investigated system is known from either experiment or computational studies applying other methods. It would be, however, desirable to apply the *orbital-free embedding* type of calculations also to optimize the geometry of the embedded subsystem without relying on structural data obtained from other methods.

Studying the applicability of the subsystem formulation of density functional theory to derive equilibrium geometries is made here not only for the outlined pragmatic reasons. Whereas the errors in the total energy originate from the errors in the functionals and their derivatives, the errors in the equilibrium geometry originate only from the fact that the functional derivatives (effective potentials) of the relevant density functionals are not exact. We note that the errors in electron density and all one-electron properties also depend only on the quality of the effective potentials.

Opposite to the Kohn−Sham formulation of DFT, not a single reference system of noninteracting electrons but several such artificial systems are considered in the subsystem formulation of DFT.[9] As a consequence, different components of the total energy are approximated by means of explicit density functionals than in calculations based on the Kohn−Sham framework. In the subsystem formulation of DFT, the approximated components include exchange-correlation energy and a small part of the kinetic energy (nonadditive kinetic energy). Both local density approximation (LDA) and generalized gradient approximation (GGA) types of functionals for the kinetic energy component have been used/tested.[11] Using LDA functionals for all relevant energy contributions in subsystem formulation of DFT results in a computational method which is entirely parameter-free. In previous computational studies of weakly bound intermolecular complexes, which focused mainly on interaction energies, this approximation proved to be very good for hydrogen-bonded complexes[12] as well as a number of other complexes formed by atoms or nonpolar molecules Ne−Ne, F_2−Ne, N_2−N_2, N_2−Ar, Ar−Ar, and CH_4−CH_4, for instance.[13] For a large class of weak intermolecular complexes, however, such as diatomic molecules interacting with benzene,[14] benzene dimer,[15] C_3H_6−Ar, C_6H_6−Ar, C_6H_6−CH_4, C_6H_6−C_2H_6, C_3H_8−C_3H_8, C_6H_6−C_2H_4, and C_6H_6−C_2H_2,[13] LDA leads to unsatisfactory results. As a rule of thumb, LDA fails in obtaining interaction energies if π-systems are involved in the intermolecular interaction.[16] For such a system, a particular combination of gradient dependent functionals of the GGA type proposed and tested for the first time in ref 14 improves the interaction energies qualitatively. Unfortunately, this approximation worsens the interaction energies in the case of systems for which LDA is adequate. We underline that opposite to the LDA case, the GGA functionals are not defined uniquely. In our choice for GGA functionals, motivated by their properties, the nonadditive kinetic energy is approximated using such a GGA functional, which leads to the best associated functional derivative in the case of weakly overlapping pairs of electron densities.[11] As far as the exchange-correlation component is concerned, the chosen approximation is the functional of Perdew and Wang,[17,18] which has the most similar analytic form to the one for the kinetic energy part and satisfies the Lieb-Oxford condition.[19]

It is worthwhile to recall that in the original applications of the subsystem formulation of density functional theory to ionic solids, the subsystems corresponded to atoms and the LDA functionals were used together with additional approximations on the symmetry and localization of orbitals for each subsystem.[9,20] In our adaptation of this formalism to molecular systems, LDA and GGA functionals can be used, and no restrictions are made on symmetry or localization of orbitals in each subsystem.[8]

The above numerical results concerning applicability of LDA and GGA functionals in the subsystem formulation of DFT leave us, therefore, with a number of questions of practical importance such as the following: (i) In which class of systems LDA can be reliably applied to obtain interaction energies? (ii) In which class of systems GGA can be reliably applied to obtain interaction energies? (iii) How good are LDA and GGA equilibrium geometries?

LDA applied in the Kohn−Sham framework to approximate the exchange-correlation energy is known to lead to rather unsatisfactory interaction energies for weakly bound intermolecular complexes. Therefore, the good performance of LDA applied to both exchange-correlation and nonadditive kinetic energy functionals in the subsystem formulation of DFT indicates that errors in the corresponding functionals cancel each other to some extent. This brings up additional intriguing questions of a more fundamental nature: (iv) What

are the physical conditions for such a cancellation to take place? (v) How to construct conjoint gradient-dependent approximations to the exchange-correlation- and nonadditive kinetic energies assuring that such cancellation is maximal?

Moreover, since the overall accuracy of the interaction energy is determined by the errors in two types of quantities, functionals and their functional derivatives, it is important to assess the quality of these quantities independently for each considered approximation.

In this work, we report the results of numerical analysis addressing some of the above practical issues in detail. To this end, the equilibrium geometries are in focus of our analysis. The quality of this property is determined by the functional derivatives of the approximated density functionals. The practical importance of determining the range of applicability of LDA and GGA are obvious. This work complements the recently reported analysis of the interaction energies[16] calculated at equilibrium geometries obtained from benchmark wavefunction based calculations.

As far as accuracy of the kinetic-energy-functional dependent energy component is concerned, the Kohn−Sham results (LDA and GGA) are also discussed in this work. In the applied computational scheme, any differences between Kohn−Sham and subsystem-based calculations can be attributed to this functional (and its derivative).

For some intermolecular complexes of high symmetry, we reported already the equilibrium geometries derived from subsystem based calculations applying the functionals of the LDA and GGA type. The recent numerical implementation of the formalism makes it possible to study systems with more degrees of freedom such as the ones in the Zhao and Truhlar data set comprising equilibrium geometries and interaction energies for a group of representative intermolecular complexes,[21] obtained by means of a high-level wave function based type of calculations and intended to be used as a benchmark. These authors used the same reference data to assess the performance of various approximations to the exchange-correlation energy functional applied within the Kohn−Sham framework.

The complexes in the test set are divided into the following groups:[22,23]

- *hydrogen bonded* (HB6/04) NH_3-NH_3, HF−HF, H_2O-H_2O, NH_3-H_2O, $HCONH_2-HCONH_2$, and HCOOH−HCOOH,
- *dominated by dipolar interactions* (DI6/04): H_2S-H_2S, HCl−HCl, H_2S−HCl, CH_3Cl−HCl, HCN−CH_3SH, and CH_3SH−HCl,
- *weakly bonded* (WI9/04): He−Ne, He−Ar, Ne−Ne, Ne−Ar, CH_4−Ne, C_6H_6−Ne, CH_4-CH_4, $C_2H_2-C_2H_2$, and $C_2H_4-C_2H_4$. It is worthwhile to underline that the strength of intermolecular interactions varies in a wide range (up to about 16 kcal/mol).

The numerical differences between our results and that in the compared database can be attributed to three factors: (i) the used basis sets, (ii) numerical procedures, and (iii) the approximations to the relevant density functionals. The errors due to the first two factors can be easily controlled and reduced in our implementation of the formalism. The effect of using approximated functionals instead of the exact ones requires, however, dedicated studies on a case by case basis such as the ones reported in the present work.

2. Methods

2.1. The Subsystem Formulation of Density Functional Theory. In the subsystem formulation of density functional theory,[9] several sets of one-electron functions are used to construct the electron density of each subsystem. Within each set, the one-electron functions are orthogonal.

In the particular case of two subsystems, considered here, a natural choice of the subsystems corresponds to individual molecules forming the complex. The key quantity in this formulation of DFT is the functional referred to here as Ξ^S, which depends explicitly on two sets of one-electron functions ($\{\phi_i^A\}$, $i = 1, N^A$, $\{\phi_i^B\}$, $i = 1, N^B$) and reads as

$$\Xi^S[\{\phi_i^A\},\{\phi_i^B\}] = V[\rho_A + \rho_B] + J[\rho_A + \rho_B] + E_{xc}[\rho_A + \rho_B] + 2\sum_{i=1}^{N^A}\left\langle \phi_i^A \middle| -\frac{1}{2}\nabla^2 \middle| \phi_i^A \right\rangle + 2\sum_{i=1}^{N^B}\left\langle \phi_i^B \middle| -\frac{1}{2}\nabla^2 \middle| \phi_i^B \right\rangle + T_s^{nad}[\rho_A,\rho_B] \quad (1)$$

where

$$\rho_A = 2\sum_{i=1}^{N^A}|\phi_i^A|^2 \qquad \rho_B = 2\sum_{i=1}^{N^B}|\phi_i^B|^2 \quad (2)$$

The density functionals $E_{xc}[\rho]$, $J[\rho]$, and $V[\rho]$, represent exchange-correlation energy, the Coulomb repulsion, and the energy of the interaction with external field (nuclei), respectively. These functionals are defined in the same way as in the Kohn−Sham formulation of DFT. The bifunctional $T_s^{nad}[\rho_A,\rho_B] = T_s[\rho_A + \rho_B] - T_s[\rho_A] - T_s[\rho_B]$ is expressed by means of the density functional of the kinetic energy in the reference system of noninteracting electrons ($T_s[\rho]$).[24] In practical calculations based on the Kohn−Sham formalism, the numerical value of $T_s[\rho]$ is available at the end of the self-consistent procedure without relying on any approximated functionals. In calculations based on the subsystem formulation of DFT, only the embedded orbitals are available. They are used to calculate the exact values of $T_s[\rho_A]$ and $T_s[\rho_B]$. The numerical value of the total kinetic energy $T_s[\rho_A + \rho_B]$ is constructed using the exact results for $T_s[\rho_A]$ and $T_s[\rho_B]$ and the $T_s^{nad}[\rho_A,\rho_B]$ term, which is calculated by means of an approximated functional depending explicitly on two electron densities.

The functional $\Xi^S[\{\phi_i^A\},\{\phi_i^B\}]$ is related to the Hohenberg−Kohn energy functional $E^{HK}[\rho]$:[25]

$$E^{HK}[\rho_A + \rho_B] = \min_{\{\phi_i^A\}\to\rho_A}\min_{\{\phi_i^B\}\to\rho_B}\Xi^S[\{\phi_i^A\},\{\phi_i^B\}] = \min_{\{\phi_i^A\}\to\rho_A}\Xi^E[\{\phi_i^A\},\rho_B] \le \Xi^E[\{\phi_i^A\},\rho_B] \le \Xi^S[\{\phi_i^A\},\{\phi_i^B\}] \quad (3)$$

The equality is reached for the orbitals, obtained in the constrained search definition of $T_s[\rho]$[24] provided the total

electron density $\rho_A + \rho_B$ is v-representable, i.e., the $E^{\mathrm{HK}}[\rho_A + \rho_B]$ exists (for a complete discussion of the relation between the universal functionals in Hohenberg−Kohn theorem and their counterparts defined in constrained search see ref 26).

Euler−Lagrange minimization of $\Xi^E[\{\phi_i^A\},\rho_B]$ with respect to $\{\phi_i^A\}$ leads to one-electron equations[1]

$$\left[-\frac{1}{2}\nabla^2 + v_{\mathrm{eff}}^{\mathrm{KSCED}}[\rho_A,\rho_B]\right]\phi_i^A = \epsilon_i^A\,\phi_i^A \quad i = 1, N^A \qquad (4)$$

where

$$v_{\mathrm{eff}}^{\mathrm{KSCED}}[\rho_A,\rho_B](\vec{r}) = v_{\mathrm{eff}}^{\mathrm{KS}}[\rho_A + \rho_B](\vec{r}) + \left.\frac{\delta T_s^{\mathrm{nad}}[\rho,\rho_B]}{\delta\rho(\vec{r})}\right|_{\rho=\rho_A} \qquad (5)$$

The label KSCED (Kohn−Sham Equations with Constrained Electron Density) is used here to indicate that the multiplicative potential and the obtained one-electron functions differ from the corresponding quantities in the Kohn−Sham framework.

To facilitate comparisons with other embedding approaches, it is convenient to split $v_{\mathrm{eff}}^{\mathrm{KSCED}}$ into two components: the Kohn−Sham effective potential for the isolated subsystem A (ρ_B-independent terms) and the remaining part representing the effect of the environment (all ρ_B-dependent terms)

$$v_{\mathrm{eff}}^{\mathrm{KSCED}}[\rho_A,\rho_B](\vec{r}) = v_{\mathrm{eff}}^{\mathrm{KS}}[\rho_A](\vec{r}) + v_{\mathrm{emb}}^{\mathrm{KSCED}}[\rho_A,\rho_B](\vec{r}) \qquad (6)$$

where

$$v_{\mathrm{eff}}^{\mathrm{KS}}[\rho_A](\vec{r}) = v_{\mathrm{ext}}^{A}(\vec{r}) + \int\frac{\rho_A(\vec{r}\,')}{|\vec{r}\,' - \vec{r}|}d\vec{r}\,' + \left.\frac{\delta E_{\mathrm{xc}}[\rho]}{\delta\rho(\vec{r})}\right|_{\rho=\rho_A} \qquad (7)$$

and

$$v_{\mathrm{emb}}^{\mathrm{KSCED}}[\rho_A,\rho_B](\vec{r}) = v_{\mathrm{ext}}^{B}(\vec{r}) + \int\frac{\rho_B(\vec{r}\,')}{|\vec{r}\,' - \vec{r}|}d\vec{r}\,' + \left.\frac{\delta E_{\mathrm{xc}}[\rho]}{\delta\rho(\vec{r})}\right|_{\rho=\rho_A+\rho_B} - \left.\frac{\delta E_{\mathrm{xc}}[\rho]}{\delta\rho(\vec{r})}\right|_{\rho=\rho_A} + \left.\frac{\delta T_s^{\mathrm{nad}}[\rho,\rho_B]}{\delta\rho(\vec{r})}\right|_{\rho=\rho_A} \qquad (8)$$

Note that it is sufficient to know the electron density of the environment ρ_B to express the embedding potential given in eq 8. No information about the orbital structure of the environment is needed. For this reason, we refer to calculations using eq 8 as *orbital-free embedding*. The results of embedding calculations depend, however, on the choice made for ρ_B. In this work, ρ_B and ρ_A are treated at the same footing, as in the original subsystem formulation of DFT by Cortona. The two sets of orbitals $\{\phi_i^A\}$ and $\{\phi_i^B\}$ minimizing $\Xi^S[\{\phi_i^A\},\{\phi_i^B\}]$ satisfy two sets of coupled equations

$$\left[-\frac{1}{2}\nabla^2 + v_{\mathrm{eff}}^{\mathrm{KSCED}}[\rho_A,\rho_B]\right]\phi_i^A = \epsilon_i^A\,\phi_i^A \quad i = 1, N^A \qquad (9)$$

$$\left[-\frac{1}{2}\nabla^2 + v_{\mathrm{eff}}^{\mathrm{KSCED}}[\rho_B,\rho_A]\right]\phi_i^B = \epsilon_i^B\,\phi_i^B \quad i = 1, N^B \qquad (10)$$

where the electron densities and orbitals are related via eq 2.

At a given external field (geometry of nuclei), minimization of the total energy with respect to ρ_A and ρ_B can be obtained in a self-consistent procedure (*freeze-and-thaw*[8]), in which eqs 9 and 10 are solved consecutively until convergence. In this way, the fully variational calculations based on the subsystem formulation of DFT are formulated as a self-consistent series of *orbital-free embedding* calculations.

The orbitals derived from eqs 9 and 10 ($\phi_{i(o)}^A$ and $\phi_{i(o)}^B$) yield the electron densities ρ_A^o and ρ_B^o. By construction, ρ_A^o and ρ_B^o are pure-state noninteracting v-representable. Therefore,

$$T_s[\rho_A^o] = 2\sum_{i=1}^{N^A}\left\langle\phi_{i(o)}^A\right| -\frac{1}{2}\nabla^2\left|\phi_{i(o)}^A\right\rangle \qquad (11)$$

$$T_s[\rho_B^o] = 2\sum_{i=1}^{N^B}\left\langle\phi_{i(0)}^B\right| -\frac{1}{2}\nabla^2\left|\phi_{i(o)}^B\right\rangle \qquad (12)$$

In such a case, the right-hand side of eq 1 evaluated for $\phi_{i(o)}^A$ and $\phi_{i(o)}^B$ equals exactly to $E^{\mathrm{HK}}[\rho_A^o + \rho_B^o]$.

2.2. Approximations for $E_{\mathrm{xc}}[\rho]$ and $T_s^{\mathrm{nad}}[\rho_A,\rho_B]$. In this work, LDA and GGA density functionals are considered. We will use the labels KSCED LDA and KSCED GGA for the corresponding computational methods, in which the total energy of the intermolecular complex is evaluated from eq 1 and the embedded orbitals are obtained from eqs 9 and 10.

In the KSCED LDA calculations, the exchange functional is approximated using the expression for the uniform gas of noninteracting electrons by Dirac,[27] the correlation energy is approximated using the Vosko et al.[28] parametrization (eq 4.4 in ref 28 referred frequently as "VWN V") of the Ceperley-Alder[29] reference data for correlation energy in the uniform electron gas, and the nonadditive kinetic energy is approximated using the Thomas-Fermi formula for the kinetic energy.[30,31] Note that the above approximate functionals do not rely on any empirical data.

In the KSCED GGA calculations, the Perdew−Wang (PW91)[17,18] exchange-correlation functional is used, whereas the nonadditive kinetic energy bifunctional $T_s^{\mathrm{nad}}[\rho_A,\rho_B]$ is approximated according to the formula: $T_s^{\mathrm{nad}}[\rho_A,\rho_B] \approx T_s^{\mathrm{nad(GGA97)}}[\rho_A,\rho_B] = T_s^{\mathrm{LC94}}[\rho_A + \rho_B] - T_s^{\mathrm{LC94}}[\rho_A] - T_s^{\mathrm{LC94}}[\rho_B]$, where $T_s^{\mathrm{LC94}}[\rho]$ denotes the Lembarki-Chermette[32] functional of the kinetic energy. The $T_s^{\mathrm{nad(GGA97)}}[\rho_A,\rho_B]$ was shown to provide a good approximation to the nonadditive kinetic energy potential in the case of weakly overlapping densities.[11,33]

2.3. Energy Minimization. The local minimum at the Born−Oppenheimer potential energy surface corresponds to a minimum of the functional $\Xi^S[\{\phi_i^A\},\{\phi_i^B\}]$ with respect to several independent quantities: positions of nuclei in each subsystem $\{\mathbf{R}_A\}$ and $\{\mathbf{R}_B\}$ (geometrical degrees of freedom) and two electron densities ρ_A and ρ_B (electronic-structure related degrees of freedom). The electronic energy in the Born−Oppenheimer approximation corresponds to the numerical value of the Hohenberg−Kohn total energy functional $E^{\mathrm{HK}}[\rho_A^o + \rho_B^o]$. All quantities needed to evaluate

Table 1. Considered Optimization Schemes

label	optimized	frozen	treatment of ρ_A and ρ_B
A	$\{\mathbf{R}_A\}$, ρ_A, $\{\mathbf{R}_B\}$, ρ_B		fully variational[8,9]
B	$\{\mathbf{R}_A\}$, ρ_A, ρ_B	$\{\mathbf{R}_B\}$	fully variational[8,9]
C	ρ_A, ρ_B	$\{\mathbf{R}_A\}$, $\{\mathbf{R}_B\}$	fully variational[8,9]
D	$\{\mathbf{R}_A\}$, ρ_A	$\{\mathbf{R}_B\}$, ρ_B	partially variational[1]
E	ρ_A	$\{\mathbf{R}_A\}$, $\{\mathbf{R}_B\}$, ρ_B	partially variational[1]
F	$\{\mathbf{R}_A\}$, $\{\mathbf{R}_B\}$	ρ_A, ρ_B	nonvariational (frozen)[44]
G		$\{\mathbf{R}_A\}$, $\{\mathbf{R}_B\}$, ρ_A, ρ_B	nonvariational (frozen)[44]

$E^{\mathrm{HK}}[\rho_A^o + \rho_B^o]$ and its gradients with respect to nuclear positions are available at the end of the *freeze-and-thaw* procedure (schemes *A*−*C* in Table 1).

If, however, only one component of the electron density (say ρ_A) is subject to optimization (eq 4), whereas ρ_B is not (schemes *D* and *E* in Table 1), eq 1 provides the upper bound for the electronic energy in the Born−Oppenheimer approximation

$$E^{\mathrm{HK}}[\rho_A^o(B) + \rho_B] \geq E^{\mathrm{HK}}[\rho_A^o + \rho_B^o] = E^{\mathrm{HK}}[\rho_{AB}^o] \quad (13)$$

where $\rho_A^o(B)$ denotes the electron density obtained from eq 4, in which a given ρ_B is used. On the virtue of the second Hohenberg−Kohn theorem, the equality is reached only if the assumed ρ_B added to $\rho_A^o(B)$ equals the ground-state electron density at this geometry (ρ_{AB}^o). Nevertheless, the orbitals obtained from eq 4 provide all necessary quantities to evaluate the numerical value of $E^{\mathrm{HK}}[\rho_A^o(B) + \rho_B] - E^{\mathrm{HK}}[\rho_B]$ and its gradients with respect to the coordinates of the nuclei in the subsystem *A*. Therefore, it is possible to optimize the geometry of subsystem *A* with frozen geometrical and electronic degrees of freedom of the subsystem *B* (scheme *D* in Table 1). For an assumed ρ_B its adequacy can be controlled by comparing the results obtained from schemes *D* and *B* (or *E* and *C* if the geometry is not the subject of investigation).

We notice also that the Gordon−Kim model[34,35] (schemes *F* and *G* in Table 1) represents an extremely simplified optimization scheme, in which changes of ρ_A and ρ_B associated with intersubsystem degrees of freedom are not taken into account. Such a scheme is only applicable in some cases (rare gas dimers, for instance). For molecules, neglecting the complexation induced changes of the electron density is not a universally adequate approximation as reported previously.[12,13]

Our numerical implementation of eqs 9 and 10 makes it possible to perform the total energy optimization following each of the schemes listed in Table 1.

In this work, we focus on the adequacy of the used approximations to $E_{\mathrm{xc}}[\rho]$ and $T_s^{\mathrm{nad}}[\rho_A,\rho_B]$ functionals for obtaining equilibrium geometries. Therefore, scheme *A* (full optimization including geometrical and electronic degrees of freedom) is applied. In our previous works, concerning the interaction energies at some representative points at the potential energy surface, scheme *C* was applied.[12,13,16] We perform the search for the local minima in the vicinity of the reference equilibrium structures taken from the data set of Zhao and Truhlar. The equilibrium geometries are obtained following an efficient minimization procedure, in which the structural and electronic degrees of freedom are optimized simultaneously (sequence II in Table 2). For each geometry update either eq 9 or 10 is solved only once. Until the equilibrium energy is reached, the numerical value of $E^{\mathrm{HK}}[\rho_A^o(B) + \rho_B]$ (or $E^{\mathrm{HK}}[\rho_A + \rho_B^o(A)]$) does not correspond to the electronic energy in the Born−Oppenheimer approximation. Obtaining this energy at intermediate geometries would require performing the *freeze-and-thaw* procedure (see sequence I in Table 2). Typically, the *freeze-and-thaw* procedure involves solving the pair of eqs 9 and 10 two or three times. Therefore, sequence II can be expected to reduce the computational effort by about a factor of 5. In this work, we consider also an even more simplified optimization procedure, in which the exchange-correlation and nonadditive kinetic energy functionals are linearized in either ρ_A (eq 9) or in ρ_B (eq 10). The errors associated with the linearization are small, and they disappear by construction at the end of the *freeze-and-thaw* procedure[36] (and also at the end of the geometry optimization procedure). The resulting computational savings depend on the number of iterations in the self-consistent procedure to solve eq 4.

2.4. Computational Details. The calculations are carried out using our numerical implementation of the subsystem formulation of DFT (the program deMon2K-KSCED[37]) based on the program deMon2K.[38] For geometry optimization, the following deMon2K-KSCED options and parameters are applied: 10^{-6} au self-consistent field energy convergence criterion, adaptive grid (TOL=5.0E-07 "GUESS" grid[39]), and the atomic basis set MG3S[40] used within the monomer-centered expansion scheme (KSCED(m) - see below). The MG3S basis set is chosen based on our recently reported analysis[16] of the effect of changing the basis set on the interaction energies. In principle, two types of basis set expansions can be considered for orbitals corresponding to each subsystem: centered on the monomer or centered on the dimer. The corresponding calculations are labeled as KSCED(m) or KSCED(s), respectively, following the convention of ref 11. For a given choice of the atomic basis sets, the KSCED(s) scheme leads to results closer to the complete basis set limit than the KSCED(m) one. However, if the atomic basis sets are sufficiently large, as the ones chosen for these studies, the two schemes lead to very similar interaction energies.[16] For the calculation of the interaction energies on the optimized geometries, the following deMon2K-KSCED program options are applied: 10^{-6} au self-consistent field energy convergence criterion, the pruned "MEDIUM" (75,302)p[41] grid, and the dimer-centered MG3S basis sets (KSCED(s) type of calculations).

Classical electron−electron interactions (Coulomb) are evaluated using auxiliary fitting functions referred to as GEN-A2*, which are automatically generated for any given orbital basis sets.[42] Further details concerning the formal framework of the applied computational methods and the numerical implementation can be found in refs 8, 9, and 12.

The energy derivatives with respect to the coordinates of nuclei of the subsystem *A* are calculated using the deMon2K-KSCED program and passed together with the total energy and the coordinates of the subsystem *A* to the generic limited-memory quasi-Newton code for unconstrained optimization

Table 2. Complete (Sequence I) or Partial (Sequence II) Optimization of the Total Electron Density in One Update of the Coordinates of All Atoms in the Complex[a]

sequence I	sequence II
$\overbrace{\{\mathbf{R}_B^k\},\{\mathbf{R}_A^i\},\ \underbrace{\rho_B \Longleftrightarrow \rho_A}_{\text{freeze-and-thaw}}}^{\text{Eq.9 or 10}}$	$\overbrace{\{\mathbf{R}_B^k\},\{\mathbf{R}_A^i\},\rho_B \Longrightarrow \rho_A^i}^{\text{Eq.9}}$
$\Updownarrow^{i=1,N-1}_{\text{until } \mathbf{R}_\mathrm{A} \text{ convergence}}$	$\Updownarrow^{i=1,N-1}_{\text{until } \mathbf{R}_\mathrm{A} \text{ convergence}}$
$\overbrace{\{\mathbf{R}_B^k\},\{\mathbf{R}_A^i\},\rho_A,\rho_B \Longrightarrow \{\mathbf{R}_A^{i+1}\}}^{\text{L-BFGS}}$	$\overbrace{\{\mathbf{R}_B^k\},\{\mathbf{R}_A^i\},\rho_A^i,\rho_B \Longrightarrow \{\mathbf{R}_A^{i+1}\}}^{\text{L-BFGS}}$
$\overbrace{\{\mathbf{R}_B^k\},\{\mathbf{R}_A^N\},\ \underbrace{\rho_A \Longleftrightarrow \rho_B}_{\text{freeze-and-thaw}}}^{\text{Eq.10 or 9}}$	$\overbrace{\{\mathbf{R}_B^k\},\{\mathbf{R}_A^N\},\rho_A^N \Longrightarrow \rho_B^k}^{\text{Eq.10}}$
$\Updownarrow^{k=1,M-1}_{\text{until } \mathbf{R}_\mathrm{B} \text{ convergence}}$	$\Updownarrow^{k=1,M-1}_{\text{until } \mathbf{R}_\mathrm{B} \text{ convergence}}$
$\overbrace{\{\mathbf{R}_B^k\},\{\mathbf{R}_A^N\},\rho_A,\rho_B \Longrightarrow \{\mathbf{R}_B^{k+1}\}}^{\text{L-BFGS}}$	$\overbrace{\{\mathbf{R}_B^k\},\{\mathbf{R}_A^N\},\rho_A^N,\rho_B^k \Longrightarrow \{\mathbf{R}_B^{k+1}\}}^{\text{L-BFGS}}$

[a] The self-consistent procedure to solve eqs 9 and 10 is denoted with *freeze-and-thaw*. The procedure to update of the coordinates in one subsystem using analytic gradients obtained from eq 9 (for subsystem *A*) or eq 10 (for subsystem *B*) is denoted with L-BFGS.

L-BFGS[43] (Broyden-Fletcher-Goldfarb-Shanno) using a Perl script, which controls the optimization process. The L-BFGS algorithm uses the following two nondefault parameters: EPS = 1.0E-05 (threshold for the norm of the gradient in [hartree/bohr]) and $M = 5$ (the number of corrections used in the update of the inverse of the Hessian). Such an optimization procedure yields the precision of the intermolecular distances for the given set of molecules on the order of 0.01 Å as tested by performing optimization starting from different geometries. The applied optimization procedure is very efficient in localizing the equilibrium intermolecular distance. For all systems discussed in this study, the equilibrium geometries were obtained by performing multiple optimization runs, each starting from a different geometry of the complex. In the initial geometry, the original structure from the Zhao−Truhlar database was modified by changing the intermolecular distance (by a few Å) as well as by mutual orientation of the monomers. Such a procedure leads to almost identical final geometries (they lie within 0.01 Å). Unfortunately, such a procedure fails to localize the minimum at flat potential energy surfaces, where some degrees of freedom are associated with very small gradients such as that corresponding to a parallel displacement of one monomer in the benzene dimer.

3. Results and Discussion

3.1. Geometries: LDA. Table 3 collects the selected representative parameters describing intermolecular degrees of freedom in the considered complexes derived from KSCED LDA calculations together with the corresponding reference data. The chosen two geometrical parameters are the intermolecular distance *R* between the closest two heavy atoms in two molecules forming the complex and a representative angle describing the relative orientation of the monomers (ϕ). The labels given for the chosen angle allow one to identify it in a straightforward manner. For instance,

Table 3. Key Parameters of the Equilibrium Geometry Obtained from KSCED LDA Calculations[a]

compound	Def$_R$	R	R_{ref}	$R - R_{ref}$	Def$_\phi$	ϕ	ϕ_{ref}
NH_3-NH_3	dNN	3.14	3.27	−0.13	HNN	16	14
HF−HF	dFF	2.87	2.78	0.08	HFF	113	115
H_2O-H_2O	dOO	2.96	2.94	0.02	HOO	5	4
NH_3-H_2O	dNO	2.97	2.97	0.01	HON	5	6
$HCONH_2-HCONH_2$	dNO	2.89	2.88	0.01	ONC	114	116
HCOOH−HCOOH	dOO	2.81	2.70	0.11	OOC	127	125
H_2S-H_2S	dSS	4.03	4.12	−0.09	HSS	90	84
HCl−HCl	dClCl	3.60	3.79	−0.19	HClCl	47	8
H_2S-HCl	dSCl	3.81	3.76	0.05	HClS	92	88
$CH_3Cl-HCl$	dClCl	3.70	3.61	0.09	ClClC	81	82
$HCN-CH_3SH$	dCS	3.62	3.52	0.10	SNC	170	162
$CH_3SH-HCl$	dSCl	3.70	3.61	0.09	HClS	14	11
He−Ne	dHeNe	2.81	3.03	−0.22	-	-	-
He−Ar	dHeAr	3.16	3.48	−0.32	-	-	-
Ne−Ne	dNeNe	3.04	3.09	−0.05	-	-	-
Ne−Ar	dNeAr	3.47	3.49	−0.02	-	-	-
CH_4-Ne	dCNe	3.44	3.49	−0.05	HNeC	70	71
C_6H_6-Ne	dCNe	3.66	3.51	0.15	NeCC	79	79
CH_4-CH_4	dCC	3.61	3.61	−0.00	HCC	70	70
$C_2H_2-C_2H_2$	dCC	3.22	3.46	−0.23	CCC	122	123
$C_2H_4-C_2H_4$	dCC	3.83	3.83	0.00	CCC	80	80

[a] R (in Å) denotes the distance between the two closest heavy atoms of different monomers, and ϕ (in deg) is a representative angle determining the relative orientation between the monomers. The reference values R_{ref} and ϕ_{ref} are taken from ref 22.

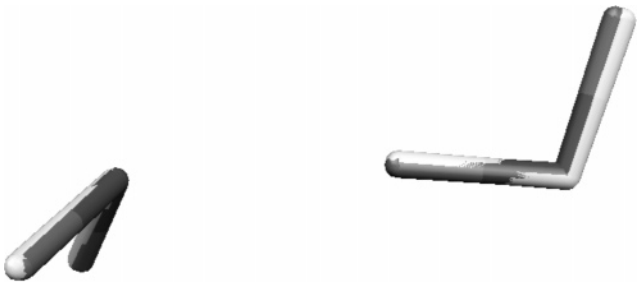

Figure 1. The optimized geometry (KSCED LDA) of the H_2O-H_2O complex superimposed on the reference equilibrium geometry (dark colors).

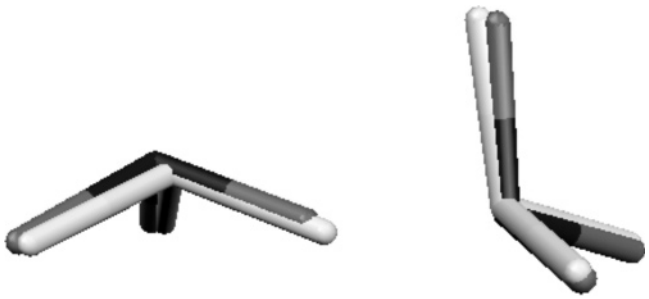

Figure 2. The optimized geometry (KSCED LDA) of NH_3-NH_3 superimposed on the reference equilibrium geometry (dark colors).

the HOO denotes the H−O−O angle in the case of the water dimer.

KSCED LDA performs very well for hydrogen-bonded complexes. This result is illustrated in Figures 1 and 2 showing the optimized geometry superimposed on the reference one for two representative complexes: H_2O-H_2O, for which KSCED LDA optimized geometry deviates the least from the reference one, and NH_3-NH_3, from which the deviation from the reference is the largest among the hydrogen-bonded complexes. The errors of intermolecular distances R are smaller than 0.10 Å for all complexes in this set except for NH_3-NH_3 and HCOOH−HCOOH. The errors in intermolecular distances tend to decrease with increasing binding energy.

In the set of the complexes of dipole character the most important difference with respect to the reference geometry is found for HCl−HCl. In the LDA optimized geometry, two monomers are in a parallel-like orientation, and in the reference one they are almost perpendicular.

For the most weakly bound systems, noticeable errors in the intermolecular distance (0.2−0.3Å) occur for He−Ne, He−Ar, and C_6H_6-Ne. Most of the intermolecular equilibrium distances in this set are underestimated, which is an opposite tendency found in the other sets.

Analyzing the overall performance of local density approximation shows that it performs very well for hydrogen-bonded complexes, which confirms the results reported elsewhere,[12] and reasonably well for weakly bound complexes. In most cases, local density approximation overestimates intermolecular distances, except for the complexes in the W9/04 set (weakly bound complexes).

Local density approximation applied within the Kohn−Sham framework leads systematically to worse results. In the case of all considered intermolecular complexes, the Kohn−Sham LDA calculations lead to underestimated intermolecular equilibrium distances. For hydrogen-bonded complexes, the errors reach −0.27 Å for NH_3-NH_3. In the case of dipole bound species, the maximal error occurs for H_2S-H_2S (−0.38 Å). Taking into account that the errors of equilibrium geometries are determined by the quality of the exchange-correlation effective potential whereas the differences between Kohn−Sham LDA and KSCED LDA results are due to the errors in the functional derivatives of the T_s^{nadd}, the superiority of KSCED LDA is the result of the compensation of errors in these quantities. For interaction energies, such compensation was reported previously for several systems[13,14] (see also below).

3.2. Geometries: GGA. KSCED GGA calculations lead to underestimated intermolecular distances for all considered complexes (see Table 4). For hydrogen-bonded complexes, the errors in intermolecular distance are larger than the ones in the KSCED LDA case reaching −0.43 Å for NH_3-NH_3. Figures 3 and 4 show the KSCED GGA optimized geometry superimposed on the reference one for two representative complexes: HCOOH−HCOOH, for which KSCED GGA optimized geometry deviates the least from the reference one, and NH_3-NH_3, for which the deviation from the reference is the largest among the hydrogen-bonded complexes.

For the dipole-bound complexes, the largest difference with respect to the reference geometry is found for HCl−HCl. As in the case of KSCED LDA equilibrium geometry, the two monomers adopt a parallel-like orientation. In this group of complexes, the errors in the intermolecular distances are rather large reaching 0.44 Å for HCl−HCl.

Table 4. Key Parameters of the Equilibrium Geometry Obtained from KSCED GGA Calculations[a]

compound	Def_R	R	R_{ref}	$R - R_{ref}$	Def_ϕ	ϕ	ϕ_{ref}
NH_3-NH_3	dNN	2.83	3.27	−0.43	HNN	40	14
HF−HF	dFF	2.73	2.78	−0.05	HFF	103	115
H_2O-H_2O	dOO	2.84	2.94	−0.10	HOO	5	4
NH_3-H_2O	dNO	2.86	2.97	−0.11	HON	6	6
$HCONH_2-HCONH_2$	dNO	2.77	2.88	−0.11	ONC	115	116
HCOOH−HCOOH	dOO	2.68	2.70	−0.02	OOC	128	125
H_2S-H_2S	dSS	3.84	4.12	−0.27	HSS	94	84
HCl−HCl	dClCl	3.35	3.79	−0.44	HClCl	46	8
H_2S-HCl	dSCl	3.62	3.76	−0.14	HClS	87	88
$CH_3Cl-HCl$	dClCl	3.49	3.61	−0.12	ClClC	78	82
$HCN-CH_3SH$	dCS	3.21	3.52	−0.31	SNC	146	162
$CH_3SH-HCl$	dSCl	3.47	3.61	−0.14	HClS	21	11
He−Ne	dHeNe	2.55	3.03	−0.48			
He−Ar	dHeAr	2.97	3.48	−0.51			
Ne−Ne	dNeNe	2.73	3.09	−0.36			
Ne−Ar	dNeAr	3.22	3.49	−0.27			
CH_4-Ne	dCNe	3.15	3.49	−0.34	HNeC	70	71
C_6H_6-Ne	dCNe	3.39	3.51	−0.12	NeCC	78	79
CH_4-CH_4	dCC	3.29	3.61	−0.33	HCC	70	70
$C_2H_2-C_2H_2$	dCC	2.95	3.46	−0.51	CCC	120	123
$C_2H_4-C_2H_4$	dCC	3.52	3.83	−0.31	CCC	79	80

[a] R (in Å) denotes the distance between the two closest heavy atoms of different monomers, and ϕ (in deg) is a representative angle determining the relative orientation between the monomers. The reference values R_{ref} and ϕ_{ref} are taken from ref 22.

In the last group of complexes (weakly bound), the errors of the KSCED GGA equilibrium intermolecular distances are very large reaching 0.51 Å.

In view of the fact that the chosen GGA functional significantly worsens the equilibrium geometry for the complexes, for which KSCED LDA leads to rather good results, this approximation does not represent a universal improvement over LDA. Since, however, it leads to significantly better binding energies for (π-stacked systems[13−15]), it can be considered as a pragmatic choice for this type of complexes.

As far as Kohn−Sham calculations are concerned, the PW91 results are significantly and systematically better then the LDA ones. For instance, the errors in the PW91 equilibrium intermolecular distances do not exceed 0.1 Å, whereas the LDA one reaches −0.27 Å for hydrogen-bonded complexes. Opposite to the tendencies discussed previously for LDA, KSCED GGA are not better than Kohn−Sham PW91 ones. The Kohn−Sham equilibrium geometries are slightly (hydrogen-bonded complexes) or noticeably (dipole bound and van der Waals) better quality than the KSCED GGA results. This indicates that the error in the PW91 exchange-correlation potential is not compensated so well with the error in the GGA97 nonadditive kinetic energy potential as it is the case of LDA.

3.3. Binding Energies at Optimized Geometries. Binding energies discussed in this section are calculated at the optimized geometries and are obtained using the dimer centered expansion of the electron density of each subsystem (KSCED(s) type of calculations). The basis set superposition error and the errors resulting from the superposition of numerical grids are taken into account following the procedure of ref 16, which is also given in the Supporting Information. We start the analysis with the LDA results. For most of the considered hydrogen-bonded complexes, the binding energies are very good. For dipole-bound complexes, the errors in the binding energy are larger. The maximal relative overestimation of the binding energy for HCN−CH_3SH reaches 30%, whereas the binding energy in CH_3Cl−HCl is underestimated by 19%. For van der Waals complexes, KSCED LDA does not perform uniformly. The interactions of helium with other atoms is overestimated significantly. The accuracy of the KSCED LDA binding energies changes from excellent to mediocre along the series, Ne−Ne, Ne−Ar, Ne−CH_4, and Ne−C_6H_6. For complexes involving saturated hydrocarbons, KSCED LDA performs reasonably well underestimating, however, the binding energy.

Results collected in Table 5 indicate clearly that the presence of a multiple bond of one molecule in the vicinity of the other molecule in the complex leads systematically to significant errors in binding energies calculated at the KSCED LDA level. Except for $C_2H_2-C_2H_2$, they are underestimated by about a factor of 2. This trend is in line with that for interaction energies calculated at reference intermolecular geometries for the same[16] or other complexes involving conjugated π systems.[13−15]

The choice of the GGA functionals (exchange-correlation- and nonadditive kinetic energies) used in this work was shown previously to lead to significant improvements of accuracy of the interaction energies in the cases where KSCED LDA fails: complexes between diatomic molecules and benzene,[14] benzene dimer,[15] and other complexes involving interactions with π bonds.[13] Results collected in Table 5 show that this choice of gradient-dependent functionals for exchange-correlation- and nonadditive kinetic energies significantly worsens this quantity for all types of complexes considered in this work.

As far as the compensation of errors in the exchange-correlation- and nonadditive kinetic energies are concerned, a similar trend (for LDA, the compensation of errors in the energies occurs systematically, whereas it is less systematic in the GGA case) can be seen as the one for the accuracy of the effective potentials discussed in the previous section. The binding energies derived from Kohn−Sham LDA calculations are significantly worse than their KSCED LDA counterparts. For all the considered complexes, the deviations from the reference data are rather large, reaching 7.75 kcal/mol for $HCONH_2-HCONH_2$ and 12.01 kcal/mol for HCOOH−HCOOH (the corresponding KSCED LDA errors are 0.09 kcal/mol and 1.72 kcal/mol) for instance. As far as GGA is concerned such systematic trends cannot be identified. On the average, the Kohn−Sham PW91 binding energies are better than KSCED GGA.

3.4. Acceleration Techniques for Geometry Optimization. In this section, we consider two optimization schemes (see Table 2) as well as their two modifications: (i) sequence I′, in which the converged *freeze-and-thaw* cycle is replaced by solving the pair or eqs 9 and 10 only once per geometry update, and (ii) a modified sequence II, in which the functional $E_{xc}[\rho_A + \rho_B] - E_{xc}[\rho_A] + T_s^{nad}[\rho_A,\rho_B]$ is linear-

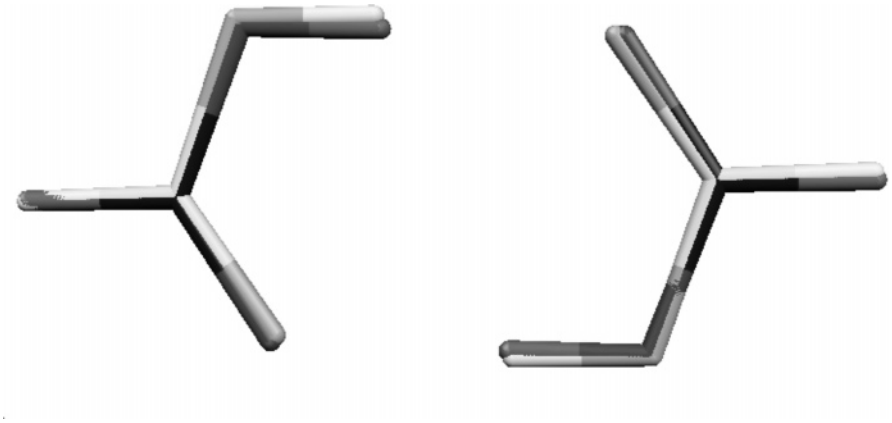

Figure 3. The optimized geometry (KSCED GGA) of the HCOOH−HCOOH complex superimposed on the reference equilibrium geometry (dark colors).

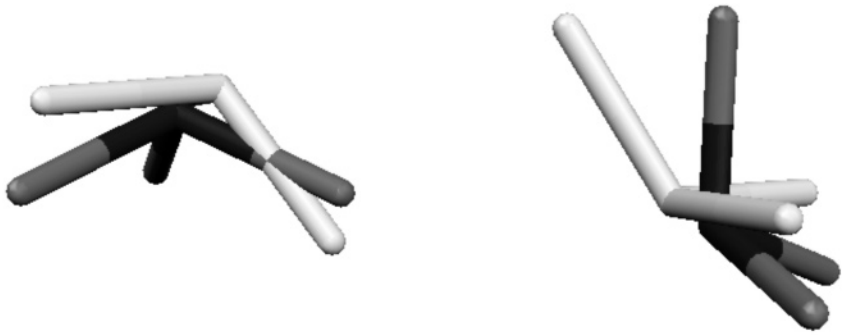

Figure 4. The optimized geometry (KSCED GGA) of NH_3-NH_3 superimposed on the reference equilibrium geometry (dark colors).

Table 5. Binding Energies ($-\Delta E$ in kcal/mol) Calculated at Optimized Geometries[a]

compound	$-\Delta E^{LDA}$		$-\Delta E^{GGA}$		$-\Delta E^{Ref}$
NH_3-NH_3	3.99	(27)	5.59	(77)	3.15
HF−HF	4.12	(−10)	5.00	(9)	4.57
H_2O-H_2O	4.97	(0)	5.94	(20)	4.97
NH_3-H_2O	6.72	(5)	8.03	(25)	6.41
$HCONH_2-HCONH_2$	15.03	(1)	17.85	(19)	14.94
HCOOH−HCOOH	14.43	(−11)	17.47	(8)	16.15
H_2S-H_2S	2.12	(28)	2.76	(66)	1.66
HCl−HCl	2.18	(8)	3.19	(59)	2.01
H_2S-HCl	3.44	(3)	4.34	(30)	3.35
$CH_3Cl-HCl$	2.89	(−19)	4.05	(14)	3.55
$HCN-CH_3SH$	4.68	(30)	5.73	(60)	3.59
$CH_3SH-HCl$	4.40	(6)	5.74	(38)	4.16
He−Ne	0.09	(125)	0.46	(1050)	0.04
He−Ar	0.15	(150)	0.47	(683)	0.06
Ne−Ne	0.08	(0)	0.52	(550)	0.08
Ne−Ar	0.12	(-8)	0.54	(315)	0.13
CH_4-Ne	0.15	(−32)	0.66	(200)	0.22
C_6H_6-Ne	0.23	(−51)	0.95	(102)	0.47
CH_4-CH_4	0.44	(−14)	1.03	(102)	0.51
$C_2H_2-C_2H_2$	1.84	(37)	2.72	(103)	1.34
$C_2H_4-C_2H_4$	1.06	(−25)	2.00	(41)	1.42

[a] The relative error (($\Delta E - \Delta E^{Ref}$)/$\Delta E^{Ref} \times 100\%$) is given in parentheses.

ized in ρ_A in the procedure to solve eq 9 in order to accelerate it (for eq 10, $E_{xc}[\rho_A + \rho_B] - E_{xc}[\rho_B] + T_s^{nad}[\rho_A,\rho_B]$ is linearized in ρ_B). By construction, linearization is exact at the end of the *freeze-and-thaw* cycle. In view of the fact that linearization might lead to noticeable savings in the computer time, it is worthwhile to investigate the effect of linearization applied without converging *freeze-and-thaw* cycle in the intermediate stages. For two intermolecular complexes (H_2O-H_2O, $HCl-CH_3SH$), performance of the four alternative optimization procedures is analyzed in either the complete or partial optimization of geometry. In the partial optimization case, the geometry of one monomer is optimized keeping the geometry of the other frozen (Scheme *B* in Table 1). In the geometry optimization, the same convergence criteria and the other optimization parameters as described in the previous section and local density approximation are applied. The starting geometries were prepared by modifying the coordinates taken from ref 21 for one molecule in the complex (the selected intermolecular degrees of freedom are given in Table 6).

In the complete optimization calculations, all four optimization schemes lead to equivalent results. The Cartesian coordinates of corresponding atoms in optimized structures differ by less than 0.01 Å. This scatter of the minimized geometries corresponds to the precision of the optimization procedure itself. The key geometrical parameters obtained in the partial optimization (rigid geometry of one monomer) are collected in Table 6. All simplified schemes lead to the optimized geometries, which do not differ significantly from that derived using the Born−Oppenheimer surface type of optimization (sequence I in Table 2).

Table 6. Key Parameters of the Equilibrium Geometry Obtained Using Four Optimization Procedures Considered in the Text[a]

compound/parameter		sequence I	sequence I′	sequence II	sequence II linearized
H_2O-H_2O	dOO	2.95	2.95	3.02	3.00
	HOO	6	6	6	6
$HCl-CH_3SH$	dSCl	3.66	3.69	3.76	3.77
	HClS	16	15	19	19

[a] Coordinates of only one molecule (A) in the complex (A-B) are optimized. Starting parameters: dOO: 3.38 Å, HOO: 60°, dSCl: 2.65 Å, HClS: 108°.

The computational costs of the four considered optimization schemes differ significantly. In the case of the H_2O-H_2O dimer, the most expensive one (sequence I) involves 88 geometry updates to converge the coordinates of the first subsystem and solving the pair of eqs 9 and 10 two to three times per geometry update. Sequence I′ converges after 91 geometry updates; however, the pair of eqs 9 and 10 is solved only once per geometry update. In sequence II, the number of geometry updates increases to 117 but involves solving eq 9 only once per geometry update. The most effective among the studied optimization schemes is the one in which sequence II is used and eq 9 is solved using linearized functionals. Linearization results in an additional reduction of the time of computations by 20−25% per geometry update. Optimization of geometry using this scheme involves 71 geometry updates.

4. Conclusions

The current study concerns the applicability of the subsystem formulation of density functional theory for studies of equilibrium geometries and binding energies in weakly bound intermolecular complexes. Two types of approximations are considered: (i) local density approximation, which was shown in our previous studies to lead to good binding energies in hydrogen-bonded systems[12] and several weakly bound complexes[13,16] but fails for such complexes where π-electrons are involved in the interaction,[13,14,16] and (ii) our choice for gradient dependent approximation, which improves significantly the interaction energies for cases where LDA fails.[13,14,16] In the present work, a systematic analysis of the accuracy of equilibrium geometries is made, complementing thus the previously obtained results concerning interaction energies and equilibrium geometries in complexes of high-symmetry.

Concerning the applicability of local density approximation in the subsystem formulation of DFT in deriving not only intermolecular energies but also equilibrium geometries, the present work confirms the adequacy of this approximation for hydrogen-bonded complexes (the largest deviation between calculated and reference intermolecular distance amounts to 0.13 Å for NH_3-NH_3), a group of dipole-bound complexes (the largest deviation between calculated and reference intermolecular distance amounts to 0.19 Å for HCl−HCl, for which also the relative orientation is the worst), and even very weak intermolecular complexes involving Ne, Ar, and saturated hydrocarbons. In this group of complexes, the maximal relative errors in the binding energies reach 30%, but they are significantly smaller in most cases. Using local density approximation in the subsystem formulation of DFT is, however, not recommended if the target of calculations is both the binding energy and equilibrium geometry in complexes involving molecules with conjugated bonds (benzene, ethylene). This trend is in line with our previously reported results. For the weakest bonds involving He, local density approximation leads to the parameters of the potential energy surface, of only qualitative value (binding energies are overestimated by a factor of 2 or 3 in He−Ne and He−Ar dimers, respectively, whereas the equilibrium distances are too short by 0.2−0.3 Å).

As far as the chosen gradient dependent approximation is concerned, it improves neither binding energies nor equilibrium geometries in the group of complexes for which local density approximation is adequate (hydrogen bonds, dipole-bonds, weak complexes involving, Ne, Ar, or saturated hydrocarbons). Its range of applicability is, therefore, limited to such complexes where π-electrons are involved in the interaction in line with our previously reported studies.

Owing to the mathematical structure of the subsystem formulation of density functional theory, performing simultaneous optimization of different types of degrees of freedom (electron density and nuclear coordinates in each subsystem) is straightforward. An efficient optimization scheme is proposed, in which the system reaches the minimum on the Born−Oppenheimer surface only at the end of the procedure reducing thus the computational efforts in the intermediate geometries.

This work represents an intermediate step toward development of first-principles based multilevel simulation techniques for studying electronic structure in condensed matter systems. The orbital-free embedding formalism uses functionals and potentials defined in the Kohn−Sham formulation of density functional theory. However, they are applied for other basic descriptors of the whole investigated system: the embedded orbitals for one part and electron density only for another one. In the present work, we explore the applicability of the simplest approximation—local density approximation—to derive energetic and geometrical properties of weakly interacting systems. A large class of intermolecular interactions was identified, for which LDA provides an adequate approximation to derive both the properties depending on the quality of the density functionals as well as their derivatives. In this class, the balance of approximate terms is such that the errors of the exchange-correlation- and nonadditive kinetic energy functionals cancel to a large extent. Practical applications of KSCED LDA framework in multiscale numerical studies for embedded systems interacting with their environment through interactions belonging to this class are currently carried out in our group.

As far as going beyond LDA in the subsystem formulation of DFT is concerned, the current study indicates clearly that the GGA functionals chosen based on our previous studies provide only a temporary solution for cases where LDA fails. Development of a consistent GGA approximation retaining the strengths of LDA and providing an efficient compensation of errors in gradient-dependent terms is an objective of our current studies.

Acknowledgment. The CPU computer time from the Poznań Supercomputing and Networking Center is greatly acknowledged. This work has been supported by the Swiss National Scientific Foundation.

Supporting Information Available: Optimized geometries, definitions of the labels used for intermolecular degrees of freedom, binding energies, and description of numerical implementation of the formalism. This material is available free of charge via the Internet at http://pubs.acs.org.

References

(1) Wesołowski, T. A.; Warshel, A. *J. Phys. Chem.* **1993**, *97*, 8050.

(2) Wesołowski, T. A. *J. Am. Chem. Soc.* **2004**, *126*, 11444.

(3) Neugebauer, J.; Jacob, C. R.; Wesołowski, T. A.; Baerends, E. J. *J. Phys. Chem. A* **2005**, *109*, 7805.

(4) Neugebauer, J.; Louwerse, M. J.; Belanzoni, P.; Wesołowski, T. A.; Baerends, E. J. *J. Chem. Phys.* **2005**, *123*, 114101.

(5) Jacob, C. R.; Wesołowski, T. A.; Visscher, L. *J. Chem. Phys.* **2005**, *123*, 174104.

(6) Zbiri, M.; Atanasov, M.; Daul, C.; Garcia-Lastra, J. M.; Wesołowski, T. A. *Chem. Phys. Lett*. **2004**, *397*, 441.

(7) Leopoldini, M.; Russo, N.; Toscano, M.; Dułak, M.; Wesołowski, T. A. *Chem. Eur*. J. **2006**, *12*, 2532.

(8) Wesołowski, T. A.; Weber, J. *Chem. Phys. Lett*. **1996**, *248*, 71.

(9) Cortona, P. *Phys. Rev. B* **1991**, *44*, 8454.

(10) Neugebauer, J.; Baerends, E. J. *J. Phys. Chem. A* **2006**, 8786.

(11) Wesołowski, T. A. *J. Chem. Phys.* **1997**, *106*, 8516.

(12) Kevorkyants, R.; Dułak, M.; Wesołowski, T. A. *J. Chem. Phys.* **2006**, *124*, 024104.

(13) Wesołowski, T. A.; Tran, F. *J. Chem. Phys.* **2003**, *118*, 2072.

(14) Wesołowski, T. A.; Ellinger, Y.; Weber, J. *J. Chem. Phys.* **1998**, *108*, 6078.

(15) Tran, F.; Weber, J.; Wesołowski, T. A. *Helv. Chim. Acta* **2001**, *84*, 1489.

(16) Dułak, M.; Wesołowski, T. A. *J. Mol. Mod.* **2007**, *13*, in press.

(17) Perdew, J. P.; Chevary, J. A.; Vosko, S. H.; Jackson, K. A.; Pederson, M. R.; Singh, D. J.; Fiolhais, C. *Phys. Rev. B* **1992**, *46*, 6671.

(18) Perdew, J. P.; Chevary, J. A.; Vosko, S. H.; Jackson, K. A.; Pederson, M. R.; Singh, D. J.; Fiolhais, C. *Phys. Rev. B* **1993**, *48*, 4978.

(19) Lieb, E. H.; Oxford, S. *Int. J. Quantum Chem.* **1981**, *19*, 427.

(20) Cortona, P.; Monteleone, A. V. *J. Phys.: Condens. Matter* **1996**, *8*, 8983.

(21) Zhao, Y.; Truhlar, D. G. *J. Chem. Theory Comput*. **2005**, *1*, 415.

(22) Zhao, Y.; Truhlar, D. G. *J. Phys. Chem. A* **2005**, *109*, 5656.

(23) Zhao, Y.; Truhlar, D. G. *Phys. Chem. Chem. Phys.* **2005**, *7*, 2701.

(24) Levy, M. *Proc. Natl. Acad. Sci. U.S.A.* **1979**, *76*, 6062.

(25) Wesołowski T. A. *One-electron equations for embedded electron density: challenge for theory and practical payoffs in multi-level modelling of soft condensed matter*; volume X of *Computational Chemistry: Reviews of Current Trends*; Leszczynski, J., Ed.; World Scientific: 2006; pp 1−82.

(26) van Leeuwen, R. *Adv. Quantum Chem.* **2003**, *43*, 25.

(27) Dirac, P. A. M. *Proc. Cambridge Philos. Soc.* **1930**, *26*, 376.

(28) Vosko, S. H.; Wilk, L.; Nusair, M. *Can. J. Phys.* **1980**, *58*, 1200.

(29) Ceperley, D. M.; Alder, B. J. *Phys. Rev. Lett*. **1980**, *45*, 566.

(30) Thomas, L. H. *Proc. Cambridge Philos. Soc.* **1927**, *23*, 542.

(31) Fermi, E. *Z. Phys.* **1928**, *48*, 73.

(32) Lembarki, A.; Chermette, H. *Phys. Rev. A* **1994**, *50*, 5328.

(33) Wesołowski, T. A.; Chermette, H.; Weber, J. *J. Chem. Phys.* **1996**, *105*, 9182.

(34) Massey, H. S. W.; Sida, D. W. *Philos. Mag*. **1955**, *46*, 190.

(35) Gordon, R. G.; Kim, Y. S. *J. Chem. Phys.* **1972**, *56*, 3122.

(36) Dułak, M.; Wesołowski, T. A. *J. Chem. Theory Comput.* **2006**, *2*, 1538.

(37) Dułak, M.; Wesołowski, T. A. *Int. J. Quantum Chem.* **2005**, *101*, 543.

(38) Köster, A. M.; Flores-Moreno, R.; Geudtner, G.; Goursot, A.; Heine, T.; Reveles, J. U.; Vela, A.; Salahub, D. R. deMon 2003; NRC, Canada. http://www.deMon-software.com/ (accessed Sep 8, 2006).

(39) Dułak, M.; Wesołowski, T. A. Adaptive grid technique for computer simulations of condensed matter using orbital-free embedding formalism. In *Lecture Series on Computer and Computational Sciences Vol. 3*; Simos, T., Maroulis, G., Eds.; VSP/Brill: 2005; pp 282−288.

(40) Lynch, B. J.; Zhao, Y.; Truhlar, D. G. *J. Phys. Chem. A* **2003**, *107*, 1384.

(41) Gill, P. M. W.; Johnson, B. G.; Pople, J. A. *Chem. Phys. Lett*. **1993**, *209*, 506.

(42) Köster, A. M.; Calaminici, P.; Escalante, S.; Flores-Moreno, R.; Goursot, A.; Patchkovskii, S.; Reveles, J. U.; Salahub, D. R.; Vela, A.; Heine, T. *The deMon User's Guide, Version 1.0.3, 2003−2004*. http://www.deMon-software.com/ (accessed Sep 8, 2006).

(43) Liu, D. C.; Nocedal, J. *Math. Program.* **1989**, *45*, 503.

(44) Kim, Y. S.; Gordon, R. G. *J. Chem. Phys.* **1974**, *61*, 1.

CT600367T